Anisotropic plasmas from axion and dilaton deformations

Aristomenis Donos,[a] Jerome P. Gauntlett[b] and Omar Sosa-Rodriguez[a]

[a] *Centre for Particle Theory and Department of Mathematical Sciences, Durham University,*
South Rd., Durham, U.K.

[b] *Blackett Laboratory, Imperial College,*
Prince Consort Rd., London, U.K.

E-mail: aristomenis.donos@durham.ac.uk, j.gauntlett@imperial.ac.uk,
o.f.sosa-rodriguez@durham.ac.uk

ABSTRACT: We construct black hole solutions of type IIB supergravity that are holographically dual to anisotropic plasmas arising from deformations of an infinite class of four-dimensional CFTs. The CFTs are dual to $AdS_5 \times X_5$, where X_5 is an Einstein manifold, and the deformations involve the type IIB axion and dilaton, with non-trivial periodic dependence on one of the spatial directions of the CFT. At low temperatures the solutions approach smooth domain wall solutions with the same $AdS_5 \times X_5$ solution appearing in the far IR. For sufficiently large deformations an intermediate scaling regime appears which is governed by a Lifshitz-like scaling solution. We calculate the DC thermal conductivity and some components of the shear viscosity tensor.

Contents

1 Introduction

An interesting arena for studying holography is provided by the $AdS_5 \times X_5$ class of solutions of type IIB supergravity, where X_5 is a compact five-dimensional Einstein manifold. When $X_5 = S^5$ the four-dimensional dual conformal theory (CFT) is given by $N = 4$ supersymmetric Yang-Mills theory [1]. Furthermore, when $X_5 = SE_5$, where SE_5 is Sasaki-Einstein, the four-dimensional CFT has $N = 1$ supersymmetry and, starting with the work of [2–4], there are infinite classes of examples where both the geometry is explicitly known and the dual field theory has also been identified.

The vacua of these theories have a complex modulus, given by constant values of $\tau \equiv \chi + ie^{-\phi}$, where χ and ϕ are the type IIB axion and dilaton, respectively, corresponding to the fact that τ is dual to a marginal operator in the dual field theory. For the case of $N = 4$ supersymmetric Yang-Mills theory τ is simply identified with the theta angle, θ, and coupling constant, g_{YM}, via $\tau \sim \frac{\theta}{2\pi} + i\frac{4\pi}{g_{YM}^2}$. The identification for theories with $N = 1$ supersymmetry is a little less direct due to renormalisation scales and is discussed in [2].

In this paper we will be interested in studying how the entire class of CFTs behave under deformations of τ, with the deformation having a non-trivial dependence on the spatial coordinates of the dual field theory. Such deformations trigger interesting RG flows which can, moreover, lead to novel IR ground states. Such spatially dependent deformations of CFTs are also of potential interest in seeking applications of holography with condensed matter systems. The deformations break translation invariance and hence they provide a mechanism to dissipate momentum in the field theory. This leads to finite DC conductivities and hence these deformations can be used to model various metallic and insulating behaviour (e.g. [5–11]).

An interesting setup, first studied in [12], involves a deformation in which the axion is linear in one of the spatial directions. It was shown that a novel ground state solution appears in the far IR of the RG flow which exhibits a spatially anisotropic Lifshitz-like scaling. These solutions were generalised to finite temperature in [13, 14], thus obtaining

a dual description of a strongly coupled homogeneous and spatially anisotropic plasma. One motivation for studying such plasmas is that they may provide some insights into the quark-gluon plasma that is seen in heavy ion collisions.

For the particular case of $N = 4$ SYM it has recently been shown [15] that the anisotropic plasma found in [13, 14] undergoes a finite temperature phase transition, demonstrating that the Lifshitz-like scaling ground state found in [12] is actually not realised in the far IR. A subsequent study [16] revealed additional phase transitions and it is not yet clear what the true ground state is. However, it remains plausible that the Lifshitz ground state is the true ground state for linear axion deformations which are associated with infinite classes of SE_5 and other X_5.

From a technical viewpoint the solutions involving linear axions are appealing because they can be obtained by numerically solving a system of ODEs. This is also a feature of another class of deformations by τ that were studied in [17] involving a linear dilaton. For this class it was shown that at $T = 0$ the RG flow approaches an $AdS_4 \times R$ solution[1] in the IR. Note that unlike the linear axion solutions, the dilaton becomes large in the linear dilaton solutions and hence string perturbation theory will break down for a non-compact spatial direction. Both the linear axion and the linear dilaton solutions can be viewed as special examples of "Q-lattices", introduced in [8], where one exploits a global symmetry of the gravitational theory in order to break translation invariance using a bulk matter sector while preserving translation invariance in the metric. For deformations involving τ the relevant bulk global symmetry is the $SL(2, R)$ symmetry of type IIB supergravity which acts on τ via fractional linear transformations.

Generic spatially dependent deformations of τ will lead to solutions, which we refer to as holographic τ-lattices, that involve numerically solving PDEs. While it is certainly interesting to construct such solutions and explore their properties, it is natural to first ask if the linear axion and dilaton deformations exhaust the Q-lattice constructions. In fact they do not. The bulk global $SL(2, R)$ symmetry has three different conjugacy classes of orbits and, as we will explain, the linear axion and the linear dilaton deformations are associated with the parabolic and hyperbolic conjugacy classes, respectively. This leaves deformations associated with the elliptic conjugacy class that we study here. We can easily obtain a simple ansatz for these deformations by changing coordinates in field space. Instead of the upper half plane, the new coordinates naturally parametrise the Poincaré disc and the τ-deformation of interest is obtained by taking a polar coordinate on the disc to depend linearly, and hence periodically, on one of the spatial directions.

The τ-lattice solutions of [12–14, 17] and the new ones constructed here can all be found in a $D = 5$ theory of gravity which arises as a consistent KK truncation of type IIB supergravity on an arbitrary X_5. We will introduce this $D = 5$ theory in section 2 where we will also briefly review the Lifshitz-like scaling solution found in [12]. The new holographic τ-lattices will be presented in section 3. The finite temperature solutions depend on two dimensionless parameters T/k and λ, where T is the temperature, while k

---

[1]This ground state is unstable for the case of $X_5 = S^5$ [17] and so it would be interesting to examine the associated finite temperature phase transitions generalising [15, 16].

and λ are the wave-number and strength of the τ-deformation, respectively. We show that at $T = 0$ the new τ-lattices all approach domain walls interpolating between $AdS_5 \times X_5$ in the UV and the same $AdS_5 \times X_5$ in the far IR, thus recovering full four-dimensional conformal invariance. The underlying physical reason for this is that the operator which we using to deform the CFT has vanishing spectral density at low energies for non-vanishing momentum. Similar domain walls have been seen in other settings involving deformations by marginal operators that break translation symmetry [18, 19] and, as in those examples, there is a renormalisation of relative length scales in moving from the UV to the IR.

A particularly interesting feature, for large enough values of λ, is that the solutions have an intermediate scaling regime, governed by the Lifshitz-like scaling solution found in [12]. At finite temperature this intermediate scaling appears for a range of T/k and we will show how it manifests itself in the temperature scaling of various physical quantities. For the $T = 0$ domain wall solutions the intermediate scaling will appear for a range of the radial variable. Since the Lifshitz-like scaling solution of [12] is singular the $T = 0$ domain wall RG flows can thus be viewed as a singularity resolving mechanism somewhat similar to some other singularity resolving flows, both bottom-up [23–26] and top-down [27]. An important difference is that here the RG flow is being driven by a deformation at non-vanishing momentum.

For the finite temperature plasmas we calculate some components of the shear viscosity tensor. The spin two components, $\eta_{||}$, with respect to the residual $SO(2)$ rotation symmetry, satisfy $4\pi\eta_{||}/s = 1$, where s is the entropy density, as usual [28, 29]. However, the spin one components $\eta_\perp$ behave differently. Defining $F \equiv 4\pi\eta_\perp/s$, for $T/k \gg 1$ we find $F \to 1$ while for $T/k \ll 1$ we find that F approaches a constant given by the renormalised relative length scales in the IR. For intermediate values of T/k we have $F < 1$, as seen in other anisotropic examples e.g. [17, 30–33] (see [34] for an anisotropic example where $F > 1$).

We also calculate the DC thermal conductivity of the plasmas in the anisotropic direction. Using the results of [35–38] this can be expressed in terms of black hole horizon data and we find that it has the correct scaling associated with the different scaling regimes. For $T \ll k$ the Boltzmann behaviour of the thermal resistivity, κ^{-1}, is Boltzmann suppressed, which is expected because of the absence of low-energy excitations supported at the lattice momentum in the infrared, k_{IR} [5]. By contrast in the intermediate scaling regime, the lattice deformation gives rise to the power law behaviour $\kappa \sim k^2(T/k)^{7/3}$. It is interesting to contrast these features with examples where power law behaviour occurs at low energies due to the non suppression of spectral density at finite momentum in the context of semi-local quantum critical points [5, 39].

We conclude the paper with some comments in section 4 while appendix A discusses the connection between the $SL(2, R)$ conjugacy classes and Q-lattices.

2 The setup

Our starting point is $D = 5$ Einstein gravity with a negative cosmological constant, coupled to a complex scalar, Φ, with action given by

$$S = \int dx^5 \sqrt{-g} \left(R + 12 - 2\frac{\nabla_\mu \Phi \nabla^\mu \Phi^*}{(1 - \Phi\Phi^*)^2} \right) . \tag{2.1}$$

The corresponding equations of motion are given by

$$R_{\mu\nu} + 4\, g_{\mu\nu} - 2\, \frac{\nabla_\mu \Phi \, \nabla_\nu \Phi^*}{(1 - \Phi\Phi^*)^2} = 0\,,$$

$$\nabla_\mu \left[\frac{\nabla^\mu \Phi}{(1 - \Phi\Phi^*)^2} \right] - 2\, \frac{\nabla_\mu \Phi \, \nabla^\mu \Phi^*}{(1 - \Phi\Phi^*)^3} \Phi = 0\,. \tag{2.2}$$

The complex scalar Φ parametrises the unit Poincaré disc $\mathrm{SU}(1,1)/\mathrm{U}(1) \cong \mathrm{SL}(2,R)$. It will be helpful to introduce two other standard choices of coordinates for the scalar field manifold. For the first we write

$$\Phi = \frac{1 + i\,\tau}{1 - i\,\tau}, \qquad \tau = \chi + i\, e^{-\phi}\,, \tag{2.3}$$

where ϕ is the dilaton, χ is the axion and τ parametrises the upper half plane. The metric on the scalar field manifold then takes the form

$$ds_2^2 \equiv 2 \frac{d\Phi\, d\Phi^*}{(1 - \Phi\Phi^*)^2} = \frac{d\tau d\bar{\tau}}{2(\mathrm{Im}\,\tau)^2} = \frac{1}{2}\, (d\phi^2 + e^{2\phi}\, d\chi^2)\,. \tag{2.4}$$

The second choice of coordinates

$$\Phi = \tanh\frac{\varphi}{2}\, e^{i\,\alpha}\,, \tag{2.5}$$

resembles polar coordinates with $\varphi \geq 0$ and $0 \leq \alpha < 2\pi$ parametrising a circle. The two coordinate systems are related through the non-linear field redefinition:

$$\chi = \frac{\sinh\varphi \, \sin\alpha}{\cosh\varphi + \sinh\varphi \, \cos\alpha}\,,$$

$$e^\phi = \cosh\varphi + \sinh\varphi \, \cos\alpha\,. \tag{2.6}$$

In these coordinates the metric on the scalar manifold is given by

$$ds_2^2 = \frac{2}{(1 - \Phi\Phi^*)^2}\, d\Phi\, d\Phi^* = \frac{1}{2}\, (d\varphi^2 + \sinh^2\varphi\, d\alpha^2)\,. \tag{2.7}$$

The $D = 5$ theory (2.1) is a consistent truncation of type IIB supergravity on a general five dimensional Einstein manifold X_5. In this truncation the IIB dilaton and axion are precisely χ and ϕ, respectively, while the self-dual IIB five-form is proportional to the $D = 5$ volume form plus the volume form of X_5. The consistency of the truncation means that any solution of (2.2) can be uplifted on an arbitrary X_5 to obtain an exact solution of type IIB supergravity. In particular, the unit radius AdS_5 solution, given by

$$ds_5^2 = r^2\, (-dt^2 + d\mathbf{x}^2) + \frac{dr^2}{r^2}\,, \qquad \Phi = 0\,, \tag{2.8}$$

uplifts to the vacuum $AdS_5 \times X_5$ solution type IIB supergravity and is dual to a CFT in four spacetime dimensions. Thus, the solutions of this paper are applicable to this infinite class of CFTs. For the special case when $X_5 = S^5$ the CFT is $N = 4$ supersymmetric Yang-Mills theory and when $X_5 = SE_5$ the dual CFT has $N = 1$ supersymmetry.

The complex scalar field τ is massless when expanded about the AdS_5 vacuum and is dual to an exactly marginal operator of the dual CFT. Indeed constant values of τ, which we write as $\tau^{(0)} \equiv \chi^{(0)} + i e^{-\phi^{(0)}}$, parametrise a complex moduli space of CFTs. For the special case when $X_5 = S^5$, the operators dual to χ and $e^{-\phi}$ are proportional to $\mathrm{Tr}\, F \wedge F$ and $\mathrm{Tr}\, F^2$ in $N = 4$ Yang-Mills, respectively, and furthermore, we also have a simple identification $\tau^{(0)} \sim \frac{\theta}{2\pi} + \frac{4\pi i}{g_{YM}^2}$. To be more precise using the conventions in section 4 of [14], which in particular means that for the AdS_5 vacuum solution we take $\phi^{(0)} = 0$ and identify, for $N = 4$ Yang-Mills theory,

$$\frac{1}{g_s} \tau^{(0)} = \frac{\theta}{2\pi} + \frac{4\pi i}{g_{YM}^2} \,, \tag{2.9}$$

where g_s is the string coupling constant. For general $X_5 = SE_5$ there is a less direct map because the dual field theory is described more implicitly, but nevertheless the complex modulus can easily be identified as described in [2] (see also [40]).

It is interesting to ask what happens to the field theory when we make the deformation parameter $\tau^{(0)}$ depend on some or all of the spatial coordinates, $\mathbf{x}$, of the dual field theory. At strong coupling this can be addressed by constructing holographic solutions in which the bulk τ field behaves as $\tau(\mathbf{x}, r) \to \tau^{(0)}(\mathbf{x})$ as one approaches the AdS_5 boundary at $r \to \infty$. For the case of $N = 4$ Yang-Mills theory, this deformation corresponds to a spatially dependent θ and g_{YM}^2 via (2.9) (with g_s still a constant). The most general deformation parameter $\tau^{(0)}(\mathbf{x})$ would require the solution of a system of non-linear PDEs in the bulk. However, for a particular class of boundary deformations one can maintain enough homogeneity to reduce the problem to a system of ODEs involving only the radial coordinate r. Indeed since the scalar fields parametrise a group manifold $\mathrm{SL}(2, R)$ the bulk equations of motion have a global $\mathrm{SL}(2, R)$ symmetry and hence one can consider the Q-lattice constructions described in [8].

As we explain in appendix A there are three different Q-lattice constructions, associated with the three conjugacy classes of $\mathrm{SL}(2, R)$. In each case the scalar fields trace out a one-dimensional orbit, parametrised by one of the spatial coordinates, which we take to be z. For all three cases the associated metric is anisotropic and given by

$$ds_5^2 = -U(r) \, dt^2 + \frac{dr^2}{U(r)} + e^{2 V_1(r)} \, dz^2 + e^{2 V_2(r)} \left(dx^2 + dy^2 \right), \tag{2.10}$$

with all metric components functions of r only. The hyperbolic conjugacy class is associated with a linear dilaton, namely $\chi = 0$ and $\phi = kz$, and these solutions were constructed in [17]. Solutions associated with the parabolic conjugacy class have the axion χ linear in z. These solutions were studied in [12–14] and some features will be briefly reviewed in the next subsection. The focus of this paper is solutions associated with the elliptic conjugacy class in which the field α, introduced in (2.5), is linear in the z coordinate and will be discussed in the following section.

2.1 Brief review of linear axion solutions

The solutions obtained in [12] have

$$\phi = \phi(r), \qquad \chi = a \, z \,, \tag{2.11}$$

where a is a constant, supplemented with the metric ansatz (2.10). It is simple to check that this gives a consistent non-linear ansatz for the equations of motion, leading to a system of ODEs which can be solved numerically. At the AdS_5 boundary the dilaton vanishes so that the only deformation parameter is given by a.

For the special case when $X_5 = S^5$, corresponding to $N = 4$ Yang-Mills theory, the linear axion corresponds to a θ angle in (2.9) that is linear in the z direction. Also, recalling that the $AdS_5 \times X_5$ solutions arise from $D3$-branes sitting at the apex of the metric cone over X_5, the configurations with $\chi = a\,z$ are associated with the addition of $D7$-branes that are aligned along the x, y directions as well as wrapping X_5 and are smeared along the z direction. In fact it was shown in [13] that $a = (\lambda_{tH}/4\pi)(n_{D7}/N_c)$ where n_{D7} is the uniform density of D7-branes in the z-direction, N_c is the number of $D3$-branes and λ_{tH} is the 't Hooft parameter of the dual field theory.

By analysing the system of ODEs it was shown in [12] that for any deformation parameter a there is an RG flow from AdS_5 in the UV to a Lifshitz-like scaling solution in the far IR with

$$U = \frac{12}{11}\,r^2, \qquad V_1 = \frac{2}{3}\,\ln r, \qquad V_2 = \ln r, \qquad e^\phi = r^{2/3}. \qquad (2.12)$$

Notice that the metric of this IR solution admits the spatially anisotropic scaling symmetry $(t, x, y, z) \to (\nu t, \nu x, \nu y, \nu^{2/3} z)$ with $r \to \nu^{-1} r$. On the other hand the dilaton changes under this scaling. This means that some but not all observables will exhibit this scaling behaviour. The fact that we flow to a new fixed point in the IR demonstrates that the linear axion deformation is marginally relevant.[2]

Finite temperature generalisations of these solutions were constructed and studied in some detail in [13, 14]. For the special case of uplifting these solutions on $X_5 = S^5$, an important subtlety is that in type IIB supergravity there are perturbative modes around the IR geometry (2.12) which are unstable [12] and hence, for this case, the true ground state cannot be described by the geometry (2.12). The unstable modes lie in the $\mathbf{20'}$ representation of the global SO(6) R-symmetry and the back reaction of some of them have been studied recently using an enlarged consistent Kaluza-Klein truncation, valid just for the case when $X_5 = S^5$, in [15, 16]. By constructing finite temperature solutions it was shown in [15] that there is a phase transition at finite temperature leading to a low temperature ground state geometry which was again Lifshitz-like but with different scaling exponents [15]. However, subsequent work in [16] revealed additional instabilities and the current status is that the true ground state for this case is not yet clear. On the other hand for generic X_5 manifolds the instability of [12] is not present and one can hope that (2.12) will be the true ground state for an infinite sub-class of cases.

3 A new holographic τ-lattice

We now turn our attention to a different non-linear ansatz associated with the parametrisation (2.5). It is simple to check that the ansatz for the scalars

$$\varphi = \varphi(r), \qquad \alpha = k\,z, \qquad (3.1)$$

---

[2]Note that this is also true of the linear axion solutions constructed in [9] both at vanishing and non-vanishing charge density.

combined with the metric given by (2.10) is consistent, leading to a system of ODEs. In particular, the scalar equation of motion can be written

$$\left(e^{V_1+2V_2} U \varphi'\right)' = \frac{1}{2} k^2 e^{2V_2-V_1} \sinh 2\varphi \,. \tag{3.2}$$

The boundary deformations are now given by $\lambda \equiv \varphi^{(0)}$, where $\varphi^{(0)} \equiv \varphi(r = \infty)$, and the period k. An important difference in this parametrisation of the complex scalar, compared with those in [12, 17], is that the boundary deformation is periodic in the coordinate z with period $2\pi/k$. At fixed r, as we traverse a single period in the z direction it is clear from (2.5) that we traverse a circle in the Poincaré disc centred at the origin and with radius $\tanh \frac{\varphi}{2}$. Equivalently, in terms of χ, ϕ from (2.6) this corresponds to a circle in the upper half plane centred on the imaginary axis at $e^{-\phi} = (1 + \tanh^2 \frac{\varphi}{2})/(1 - \tanh^2 \frac{\varphi}{2})$ and with radius $2 \tanh \frac{\varphi}{2}/(1 - \tanh^2 \frac{\varphi}{2})$.

Notice, in particular, for the case of $N = 4$ Yang-Mills using (2.9) we see that both couplings θ and g_{YM}^2 are modulated by the same period. We also notice that provided φ is bounded in the bulk, which will turn out to be the case in the solutions we construct, then e^ϕ is also bounded and hence string perturbation theory is not breaking down for these solutions.[3]

Like the linear axion deformation we can again interpret these deformations as arising from $D3$-branes at the apex of the metric cone over X_5 with a distribution of $D7$-branes aligned along the (x, y) directions, wrapping X_5 and smeared in the z-direction. A striking difference however is that the integral of $\chi^{(0)}$ along a period in the z-direction vanishes and so we have a distribution of both $D7$-branes and anti $D7$-branes.

Before constructing numerical solutions, we first develop some intuition about what will happen with the solutions in the two limits $\lambda \ll 1$ and $\lambda \gg 1$. For the small λ limit it is enough to examine small and static fluctuations of the scalar based on the ansatz (3.1) around the AdS_5 vacuum solution (2.8). By linearising the scalar equation of motion (3.2) we deduce that

$$\delta\phi(r) = \lambda \frac{k^2}{2 r^2} K_2\left(\frac{k}{r}\right) \,, \tag{3.3}$$

where K_2 is a Bessel function, which close to the AdS boundary gives the desired falloff:

$$\delta\varphi(r) = \lambda - \frac{\lambda k^2}{4 r^2} + \frac{\lambda k^4}{64 r^4} \left(3 - 4\gamma - 4 \ln\left(\frac{k}{2 r}\right)\right) + \cdots \,. \tag{3.4}$$

By expanding the perturbation (3.3) close to the Poincaré horizon at $r = 0$ we find

$$\delta\varphi(r) = \lambda \sqrt{\frac{\pi}{8}} \left(\frac{k}{r}\right)^{3/2} e^{-k/r} + \cdots \,. \tag{3.5}$$

This perturbation will back react on the metric at order λ^2 and explicit expressions can be obtained in terms of Meijer G-functions. The behaviour in (3.5) demonstrates that when

---

[3]Recall that we are using conventions where string perturbation theory is governed by $g_s e^\phi$, where g_s is a free constant.

λ is small, the deformation of the boundary theory does not significantly affect the IR physics away from the AdS_5 vacuum (2.8). Indeed it is clear that k sets a scale in the bulk with the geometry rapidly returning to the AdS_5 vacuum at $r < k$. At finite temperature, similar statements can be made for the corresponding horizon at temperatures $T < k$.

We conclude that at $T = 0$, at least for small λ, the deformation gives rise to a domain wall solution interpolating between AdS_5 in the UV and the same AdS_5 in the IR. This behaviour should be contrasted with what occurs for the linear axion deformations [12] and the linear dilaton deformations [17], both of which modify the lR. As we will explain in more detail later there is a renormalisation of relative length scales as one moves from the UV to IR, which for small λ is of order λ^2. Note that similar domain walls have been shown to arise in other contexts involving deformations with spatially dependent marginal operators [18, 19].

We now turn our attention to deformations corresponding to large λ. In this case, one has to construct the full geometry either in closed form or, as we do in the next section, numerically. However, we can still obtain some insight based on analytic arguments. When λ is large, the scalar field $\varphi(r)$ close to the boundary of AdS_5 will also be large. In that region, the complex scalar target space metric in the (α, φ) coordinates given in (2.7) can be approximated by

$$ds_2^2 \approx \frac{1}{2} \left(d\varphi^2 + e^{2\varphi} d\left(\frac{\alpha}{2}\right)^2 \right) , \tag{3.6}$$

which locally looks exactly like the metric (2.4) given in the (χ, ϕ) coordinates. It is natural to expect, therefore, that for the zero temperature solutions there will be a large region where the metric scales according to (2.12) while the scalar behaves as $\varphi \approx \frac{2}{3} \ln r$. As we then move deeper in the bulk geometry, the scalar becomes smaller and this approximation breaks down. It is then plausible that as soon as soon as we are in the region $r < k$, we move quickly back to the horizon of AdS_5 with the scalar behaving as in (3.3).

Similar comments apply at finite temperature. For high temperatures we expect the entropy density, s, will scale as $s \sim T^3$ corresponding to the scaling associated with the AdS-Schwarzschild black hole. This will also be the behaviour for $T \ll k$ if the solution approaches the AdS_5 to AdS_5 domain wall, which we know happens for small λ, and we will shortly see also happens for large λ. To be more precise, due to the length renormalisation we expect this behaviour for $T \ll k_{\rm IR} \equiv k/\bar{L}_1$ (with $\bar{L}_i$ defined below; see (3.13)).

In addition we expect an intermediate scaling region where s would scale according to $s \sim T^{8/3}$ associated with the finite temperature version of the scaling solution (2.12). The lower bound of this region should satisfy $1 \ll T/k_{\rm IR}$, to ensure that we are not dominated by the $T = 0$ domain wall, while the upper bound will be fixed by ensuring that we are not dominated by the high T AdS-Schwarzschild solution. A consideration of the expansions of the functions in the UV that we give below (3.7) suggests that we should have $T/k \ll e^\lambda$.

3.1 Numerical construction

We consider the ansatz for the metric given in (2.10) supplemented with the ansatz for the complex scalar Φ given by (3.1) and (2.5). After substituting into the equations of

motion (2.2) we obtain a system of ODEs for four functions, U, V_1, V_2 and φ, of the radial coordinate r. The function U satisfies a first order ODE, while the functions V_1, V_2 and φ satisfy second order ones. In order to find finite temperature solutions we use a standard double sided shooting technique which we now outline.

Close to the AdS_5 boundary, located at $r = \infty$, the expansion of the four functions has the form

$$U(r) = r^2 \left(1 - \frac{k^2 \sinh^2 \lambda}{12r^2} + \frac{\mathcal{B}_1}{r^4} + \frac{\ln r}{72r^4} k^4 \sinh^2 \lambda (2 \cosh 2\lambda + 1) + \cdots \right),$$

$$V_1(r) = \ln r + \frac{k^2 \sinh^2(\lambda)}{12r^2} + \frac{\mathcal{B}_2}{r^4} - \frac{\ln r}{72r^4} k^4 \sinh^2 \lambda (2 \cosh 2\lambda + 1) + \cdots,$$

$$V_2(r) = \ln r - \frac{k^2 \sinh^2 \lambda}{24r^2} + \frac{k^4(\cosh 2\lambda - \cosh 4\lambda) - 576\,\mathcal{B}_2}{1152r^4}$$

$$+ \frac{\ln r}{144r^4} k^4 \sinh^2 \lambda (2 \cosh 2\lambda + 1) + \cdots,$$

$$\varphi(r) = \lambda - \frac{k^2 \sinh 2\lambda}{8r^2} + \frac{\mathcal{B}_3}{r^4} - \frac{\ln r}{96r^4} k^4 (\sinh 2\lambda - 2 \sinh 4\lambda) + \cdots. \tag{3.7}$$

In particular, after fixing the scalar deformation parameter λ as well as the length scales of the asymptotic metric, we are left with the three constants of integration $\mathcal{B}_i$. Notice that if we rescale the radial coordinate $r \to \nu r$ as well as rescaling (t, x, y, z) by ν^{-1} the ansatz will be preserved by the following scaling of the UV parameters:

$$k \to \nu k, \qquad \lambda \to \lambda,$$

$$\mathcal{B}_1 \to \nu^4 \mathcal{B}_1 - \frac{(\nu k)^4}{72} \sinh^2 \lambda (2 \cosh 2\lambda + 1) \ln \nu,$$

$$\mathcal{B}_2 \to \nu^4 \mathcal{B}_2 + \frac{(\nu k)^4}{72} \sinh^2 \lambda (2 \cosh 2\lambda + 1) \ln \nu,$$

$$\mathcal{B}_3 \to \nu^4 \mathcal{B}_3 + \frac{(\nu k)^4}{96} (\sinh 2\lambda - 2 \sinh 4\lambda) \ln \nu. \tag{3.8}$$

The log terms are associated with anomalous scaling of physical quantities due to the conformal anomaly which is non-vanishing (see [14] for a related discussion).

We also demand that the solutions have a regular black hole event horizon located at some value $r = r_+$. This leads us to the following expansion near $r = r_+$:

$$U = h_{11}(r - r_+) + h_{12}(r - r_+)^2 + \ldots,$$

$$V_1 = \mathcal{H}_2 + \mathcal{H}_1(r - r_+) + h_{22}(r - r_+)^2 + \cdots,$$

$$V_2 = \mathcal{H}_3 + h_{31}(r - r_+) + \cdots,$$

$$\varphi = \mathcal{H}_4 + h_{41}(r - r_+) + \cdots. \tag{3.9}$$

The expansion is specified by four free constants $\mathcal{H}_a$, with the remaining constants h_{ij} fixed in terms of those. We find that the temperature and entropy density of the black holes are
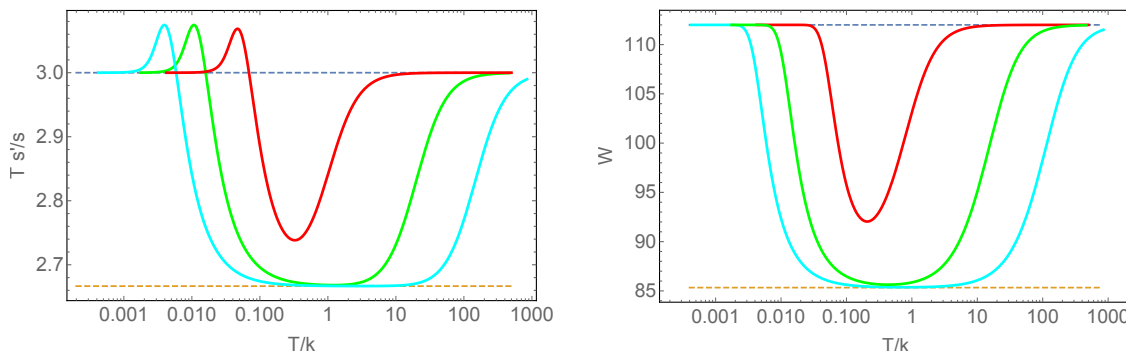
Figure 1. Plot of the function $T\,s'/s$, where s is the entropy density, and the Kretschmann scalar at the black hole horizon, W, for three values of the deformation parameter $\lambda = 2$ (red), $\lambda = 5$ (green), and $\lambda = 7$ (cyan) (the values of λ are increasing from top to bottom starting from the right of the plots). At low temperatures the solutions are approaching domain walls interpolating between AdS_5 in the UV and the same AdS_5 in the IR. The dashed constant lines in the left panel are at 3 and at 8/3, while in the right panel they are at 112 and 256/3, and the intermediate scaling behaviour, parametrically large in λ, is clearly revealed for large λ.

given by

$$
T = \frac{r_+}{\pi}\,\frac{16 + k^2(1 - \cosh(2\mathcal{H}_4))\,e^{-2\mathcal{H}_2}}{16(\mathcal{H}_1 r_+ + 1)}\,,
$$

$$
s = 4\pi e^{\mathcal{H}_2 + 2\mathcal{H}_3}\,,
\tag{3.10}
$$

respectively.

In total we have ten free constants: $\mathcal{B}_i$, λ, k, $\mathcal{H}_a$, and r_+, but one of these is redundant due to the scaling symmetry given in (3.8). By numerically solving the ODEs starting at both $r = r_+$ and $r = \infty$ we match the four functions at some point in the middle $r = r_m$ along with continuity of the first derivatives φ', V_1' and V_2'. This leads to seven conditions and thus the solution space is specified by two dimensionless parameters which we take to be λ and T/k.

We have constructed various black hole solutions for different values of the deformation parameter λ using a numerical implementation of the above technique. In figure 1 we plot the function Ts'/s as a function of T/k for three different values of λ. Notice that when Ts'/s is equal to a constant γ the entropy is scaling with temperature according to $s \propto T^\gamma$. We also plot the value of W, the Kretschmann scalar at the black hole horizon:

$$
W \equiv [R_{\mu_1\mu_2\mu_3\mu_4} R^{\mu_1\mu_2\mu_3\mu_4}]_{r=r_+}\,.
\tag{3.11}
$$

For each of the three branches we see that when $T/k \gg 1$, the entropy scales as $s \propto T^3$, as expected. Indeed, for $T/k \gg 1$ the temperature scale is much higher than the deformation scale set by λ and the solutions are approaching the standard AdS-Schwarzschild solution. This is also confirmed by the value of the Kretschmann scalar at the horizon which is approaching 112, the value for the AdS-Schwarzschild solution.

For $T/k \ll 1$, we see from figure 1 that the solutions behave similarly to the high temperature solutions. We conclude that at that low temperatures the solutions are approaching domain wall solutions that interpolate between the deformed AdS_5 in the UV and the AdS_5 vacuum in the IR. For small values of λ this was anticipated from our perturbative analysis and now we see that it also occurs for large λ.

As with other domain walls interpolating between the same AdS space (e.g. [18–22]), there can be a renormalisation of relative length scales between the UV and the IR. To extract this information we assume that the far IR of the domain wall solution at $T = 0$ has a metric as in (2.10) with $U = r^2$ and $e^{2V_i} = \bar{L}_i^2 r^2$. Since a rescaling of the radial coordinate in the IR would lead to a rescaling of both the time coordinate and the spatial coordinates, the invariant quantities, $\bar{L}_i$, are the relative length scales with respect to the scale fixed by the time coordinate. Since in the UV we approach a unit radius AdS_5, the $\bar{L}_i$ give the renormalisation of the relative length scales for the RG flow. It is slightly delicate to extract the $\bar{L}_i$ from the finite temperature solutions, because the constants $\mathcal{H}_2$ and $\mathcal{H}_3$ in (3.9) go to zero as $T \to 0$. After considering heating up the putative domain wall solution with a small temperature and examining the behaviour at the horizon, we deduce that the $\bar{L}_i$ can be obtained by taking the limit

$$\bar{L}_i = \lim_{T/k \to 0} L_i \,, \tag{3.12}$$

where we have defined[4]

$$L_i \equiv \frac{1}{\pi T} e^{V_i}|_{r=r_+} \,. \tag{3.13}$$

Since e^{V_1} and e^{V_2} are the norms of the Killing vectors ∂_z and ∂_x, ∂_y, respectively, we see that we can also write the L_i in a manifestly invariant way as:

$$L_1 = 2\left(\frac{|\partial_z|}{\kappa}\right)_{r=r_+} , \qquad L_2 = 2\left(\frac{|\partial_x|}{\kappa}\right)_{r=r_+} , \tag{3.14}$$

where here (only) κ is the surface gravity of the black hole.

We have plotted L_i as a function of T/k in figure 2. We see there is a significant relative length renormalisation in the anisotropic z direction, given by $\bar{L}_1$, that appears to monotonically increase with λ. By contrast we see that $\bar{L}_2 = 1$. The meaning of this is simply that the domain wall solution at $T = 0$ will preserve the symmetry of $\mathbb{R}^{1,2}$ along the full flow. Indeed it is easy to show that setting $e^{2V_2} = U$ is a consistent truncation of the equations of motion.

Returning to figure 1, we can also see, for sufficiently large λ, the clear emergence of an intermediate scaling behaviour with $s \propto T^{8/3}$, associated with the finite temperature Lifshitz-like scaling solution (2.12) (see [12]). To quantify this, we note that for the case of $\lambda = 7$, for example, our numerics show that the minimum of the cyan curve in the left plot of 1 takes the value 2.6668 at $T/k = 3.733$. We also see that the scaling region is becoming parametrically large as λ is increased. The lower bound is roughly given by $T/k_{\text{IR}} \gtrsim 1$

---

[4]In D spacetime dimensions we would have $L_i \equiv \frac{(D-1)}{4\pi T} e^{V_i}|_{r=r_+}$.
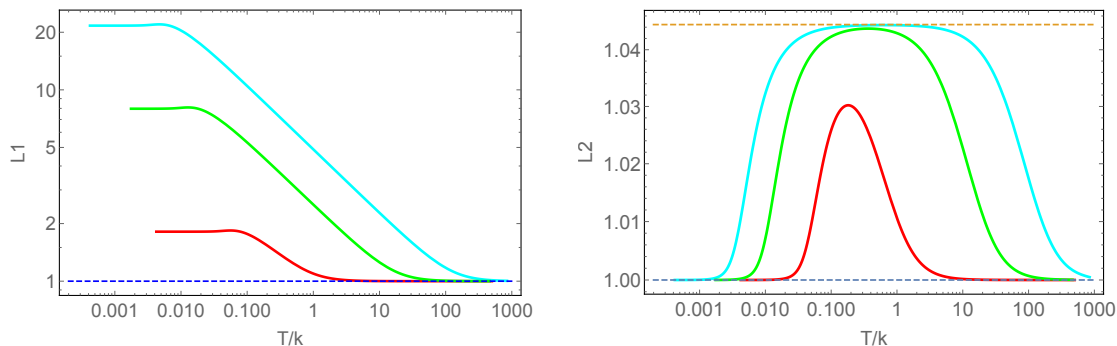
Figure 2. Plot of L_i, defined in (3.13) against T/k for three values of the deformation parameter $\lambda = 2$ (red), $\lambda = 5$ (green), and $\lambda = 7$ (cyan) (the values of λ are increasing from the bottom to the top of the plots). The values of $\bar{L}_1$ and $\bar{L}_2$, which are the values of L_1 and L_2 as $T/k \to 0$, give the relative length renormalisations in the z direction and the x, y directions, respectively, for the zero temperature AdS_5 to AdS_5 domain wall solutions. The dashed orange line at the top of the right plot is at $(12/11)^{1/2}$ associated with the intermediate scaling behaviour for large enough λ.

where $k_{\rm IR} \equiv k/\bar{L}_1$. The upper bound satisfies $T/k \ll e^\lambda$ and appears to scale with e^λ as anticipated. In the intermediate scaling region the value of the Kretschmann scalar at the horizon, W, defined in (3.11), is approaching $256/3$ which is the same as that of the black holes associated with heating up the Lifshitz-like scaling fixed point which were presented in equation (2.27) of [12]. It is also interesting to note that in the intermediate scaling regime we see from figure 2 that $L_2 \sim (12/11)^{1/2}$. This is precisely the value associated with a domain wall solution approaching (2.12) at low temperatures.

Finally, for all T/k and for all deformation parameters λ, we find that the scalar field φ monotonically decreases as a function of the radius from λ at $r = \infty$ down to a constant at the black hole horizon. This behaviour can be established by multiplying (3.2) by φ' and then integrating in the radial direction from the horizon to r. The integral of the right hand side is positive and after integrating the the left hand side by parts one can establish $(\varphi^2)' \geq 0$. Notice, in particular, that the dilaton e^ϕ is bounded and so string perturbation theory does not break down in the bulk.

3.2 Shear viscosity and DC thermal conductivity

The viscosity shear tensor, $\eta_{ij,kl}$, is defined in terms of the DC limit of the imaginary part of the retarded, two point function of the stress tensor:

$$\eta_{ij,kl} = \lim_{\omega \to 0} \frac{1}{\omega} {\rm Im} G^R_{ij,kl}(\omega) , \qquad (3.15)$$

where $G^R_{ij,kl}(\omega) = \langle T_{ij}(\omega, k = 0) T_{kl}(\omega = 0, k = 0) \rangle$. The procedure for calculating $\eta_{ij,kl}$ by studying the behaviour of metric perturbations is well known. Here we will import the results for anisotropic holographic lattices presented in [33] in order to calculate some of the components for our new anisotropic τ-lattice.

We define $\eta_{||} \equiv \eta_{xy,xy}$, which is associated with spin 2 perturbations with respect to the residual SO(2) rotation invariance in the x, y plane. By examining the behaviour of

the metric perturbation involving δg_{xy}, as in [33], we obtain the standard result

$$\eta_{\parallel} = \frac{s}{4\pi} \,. \tag{3.16}$$

We next define $\eta_{\perp} \equiv \eta_{xz,xz} = \eta_{yz,yz}$, which is associated with spin 1 perturbations with respect to SO(2). The equality arises because of the residual SO(2) rotational symmetry in the x, y plane. These components of the shear viscosity can be obtained by examining metric perturbations involving $h_{x,z}$, $h_{y,z}$ which together carry spin 1 with respect to the SO(2) symmetry. Following the calculation exactly as in [33], we obtain

$$\eta_{\perp} = \frac{s}{4\pi} \, e^{2(V_2 - V_1)}\Big|_{r=r_+} \,. \tag{3.17}$$

It is convenient to define the dimensionless quantity

$$F = \eta_{\perp} \frac{4\pi}{s} = e^{2(V_2 - V_1)}\Big|_{r=r_+} = \left(\frac{L_2}{L_1}\right)^2 \,, \tag{3.18}$$

where the L_i were defined in (3.13).

Our numerical results for F are presented in figure 3. For $T/k \gg 1$ our anisotropic solutions approach the standard AdS-Schwarzschild solution and hence in this limit we expect $F \to 1$, as we see in the figure.

Next, for $T/k \ll 1$ the solution is approaching a domain wall solution interpolating between AdS_5 in the UV and the same AdS_5 in the IR, but with a renormalisation of relative length scales. In this limit we thus expect F to approach a constant, but *a priori* it is not clear whether this constant is bigger or smaller than one. Figure 3 shows that as $T/k \to 0$ we have[5] $F \to F_0$ with $0 < F_0 < 1$. We also see that the value of F_0 monotonically decreases with increasing deformation parameter λ. Furthermore, as we decrease T/k, we see that F monotonically decreases from $F = 1$ down to $F = F_0$.

Finally, for large enough λ, in the intermediate scaling regime we expect that F will exhibit the same temperature scaling as for the Lifshitz scaling solution (2.12). An inspection of (2.12) reveals that the ratio of length scales imply $F \propto T^{2/3}$. This behaviour is also clearly visible in figure 3.

We conclude this section by calculating the DC thermal conductivity. The DC thermal conductivity is infinite in the x and y directions, due to translation invariance. However, our τ-lattice breaks translations in the z direction and hence the conductivity, κ, in this direction will be finite. It has been shown that κ can be obtained, universally, by solving a system of Stokes equations on the black hole horizon [36–38]. In fact these equations can be solved exactly for holographic lattices that depend on just one spatial direction giving results that were obtained earlier in [35]. For the case at hand we find that

$$\kappa = \frac{4\pi s T}{k^2 \sinh^2 \varphi}\Big|_{r=r_+} = \frac{16\pi^5 T^4 L_1 L_2^2}{k^2 \sinh^2 \varphi(r_+)} \,, \tag{3.19}$$

and our results are plotted in figure 4.

---

[5]This behaviour should be contrasted with the low temperature behaviour for other anisotropic models, where F is vanishing as result of different ground states at $T = 0$. For example, in the linear dilaton models $F \propto T^2$ [17], while for the linear axions solutions of [12–14] we have $F \propto T^{2/3}$ [30, 31].
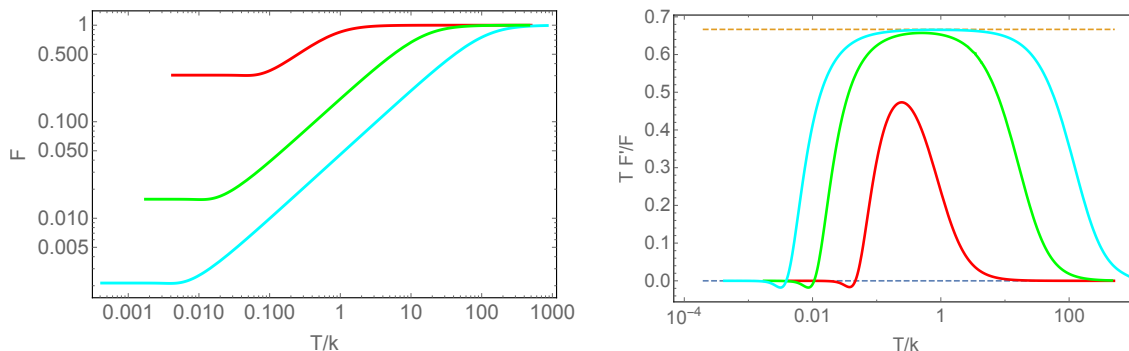
Figure 3. Behaviour of $F \equiv \eta_\perp \frac{4\pi}{s}$, where $\eta_\perp$ is a component of the shear viscosity tensor, for three values of the deformation parameter $\lambda = 2$ (red), $\lambda = 5$ (green), and $\lambda = 7$ (cyan) (the values of λ are increasing from top to bottom in the left plot and from bottom to top in the right plot). The left plot shows F monotonically decreasing from 1 at high temperatures to a non-zero constant at low temperatures. The right plot shows the intermediate scaling behaviour for large enough λ, with the dashed orange line at $2/3$.

Given the understanding of the solutions that we have now gained, for $T/k \gg 1$ we expect that the scaling with temperature of κ will be the same as for the AdS-Schwarzschild solution and hence proportional to T^4. Indeed, from (3.19), with $L_1, L_2 \to 1$ and $\varphi(r_+) \to \lambda$ we explicitly see that we have $\kappa \sim k^2(T/k)^4$ for $T/k \gg 1$.

Similarly, for $T/k \ll 1$, we expect that the system will approach an ideal conductor associated with the momentum dissipating pole for the corresponding Green's function approaching the origin in the complex frequency plane. From the perturbative solution (3.5) we can deduce that

$$\kappa \sim \frac{128\pi^7 T^7}{\lambda^2 k^5} e^{2k/\pi T}, \qquad T/k \ll 1, \qquad \lambda \ll 1. \qquad (3.20)$$

More generally by considering heating up a domain wall solution we expect $\kappa \sim (T^7/k^2 k_{\mathrm{IR}}^3)$ $\cdot e^{2k/\pi T}$ for $T/k \ll 1$.

Finally, in the intermediate scaling regime, based on the result in [35], we expect that $\kappa \sim k^2(T/k)^{7/3}$. This is exactly the behaviour that our numerics produces as we see in figure 4. For $T \ll k$ the Boltzmann behaviour of the thermal resistivity, κ^{-1}, can be understood as a consequence of the absence of low-energy excitations supported at the lattice momentum k_{IR}. More precisely, if we denote by $\mathcal{O}$ the operator dual to the axion and dilaton then the behaviour is a consequence of the vanishing of the spectral function $\mathrm{Im}\, G_{\mathcal{O}\mathcal{O}}^R(\omega, k_{\mathrm{IR}})$ as $\omega \to 0$, as explained in [5].

All of the above features for κ are clearly displayed in figure 4.

4 Discussion

We have investigated a new class of anisotropic plasmas associated with the infinite class of CFTs that have $AdS_5 \times X_5$ holographic duals. The plasmas arise from periodic deformations of the axion and dilaton of type IIB supergravity that depend on just one of the spatial
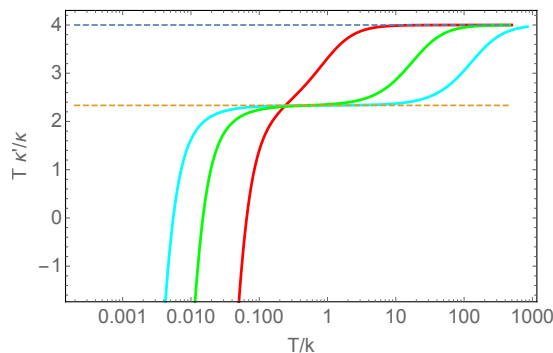
Figure 4. Behaviour of the thermal conductivity κ as a function of T/k for three values of the deformation parameter $\lambda = 2$ (red), $\lambda = 5$ (green), and $\lambda = 7$ (cyan) (the value of λ is increasing from top to bottom starting from the right of the plot). The dashed blue line is at 4 and the dashed orange line, associated with the intermediate scaling, is at $7/3$.

directions. While these deformations do not modify the far IR physics, apart from a simple renormalisation of relative lengths scales, for sufficiently large deformations there is a novel intermediate scaling regime governed by a Lifshitz-like solution with a linear axion that was found in [12].

The deformations that we have considered arise from a distribution of $D7$-branes and anti-$D7$-branes smeared along one of the spatial directions of the field theory. It is rather remarkable that one can construct back-reacted solutions for such configurations. It is also suggestive that the solutions may suffer from instabilities and it would be worthwhile to investigate this issue in more detail.

For the particular case of $X_5 = S^5$, associated with $N = 4$ Yang-Mills theory, it is known that the Lifshitz-like solution is unstable [12]. At finite temperature it was shown that the linear axion solutions have phase transitions [15, 16] leading to new branches of solutions. It would be interesting to investigate whether similar instabilities and phase transitions occur for the τ-lattices we have constructed here. It seems plausible that there is a critical value of the deformation parameter where instabilities set in. For the case of the linear axion deformations, the addition of a gauge-field has been investigated in [16, 41]. Similarly incorporating a gauge field with the new τ-lattices is another topic for further study.

The deformations that we have constructed are periodic in the spatial direction. Indeed as one moves along a period in the spatial direction the field configuration traverses a circle in the Poincaré disc. One can construct other periodic configurations by utilising the exact $\mathrm{SL}(2, Z)$ symmetry of type IIB string theory. More precisely, as one moves along a period in the spatial direction, one can demand that while τ itself is not periodic, it is periodic after acting with a non-trivial element of $\mathrm{SL}(2, Z)$. Examples of such solutions can easily be obtained from the solutions we have presented here by taking $\mathrm{SL}(2, Z)$ quotients of the circle on the Poincaré disc. Notice that integrating along the periodic spatial direction would then lead to a net (p, q) D7-brane charge. There are many more possibilities when additional spatial directions are involved and it would be interesting to explore such constructions in more detail.

A   Q-lattices and SL(2, R) conjugacy classes

The holographic lattices of [12–14, 17], and the ones studied here, are all examples of Q-lattices [8] in which one exploits the fact that the scalars parametrise the group manifold $SL(2, R)$ and consequently the gravity model admits a global $SL(2, R)$ symmetry. In particular, the spatial dependence of the scalars on the z direction is given by a specific orbit of the $SL(2, R)$ action. There are three distinct cases to consider corresponding to the three different conjugacy classes of $SL(2, R)$.

Write a general $SL(2, R)$ matrix as

$$\mathcal{M} = \begin{pmatrix} a & b \\ c & d \end{pmatrix}, \qquad ad - bc = 1. \tag{A.1}$$

The three conjugacy classes are determined by the trace: the parabolic class has $|\operatorname{Tr}\mathcal{M}| = 2$, the hyperbolic class has $|\operatorname{Tr}\mathcal{M}| > 2$ and the elliptic class has $|\operatorname{Tr}\mathcal{M}| < 2$.

The $SL(2, R)$ action on $\tau = \chi + ie^{-\phi}$ is given by $\tau \to (a\tau + b)/(c\tau + d)$. Suppose we start with $\chi = 0$ and $\phi = \phi_0$. Then acting with the one-parameter family of $SL(2, R)$ transformations in the parabolic conjugacy class given by

$$\mathcal{M} = \begin{pmatrix} 1 & kz \\ 0 & 1 \end{pmatrix}, \tag{A.2}$$

induces $\chi \to kz$ with ϕ_0 unchanged. This generates the ansatz for scalar fields given by $\phi = \phi(r)$ and $\chi = kz$ that was used in [12–14].

Next we consider the transformations in the hyperbolic conjugacy class of the form

$$\mathcal{M} = \begin{pmatrix} e^{-kz/2} & 0 \\ 0 & e^{kz/2} \end{pmatrix}. \tag{A.3}$$

This induces $\phi_0 \to \phi_0 + kz$ with $\chi = 0$ unchanged. This generates the ansatz $\phi = kz$ and $\chi = 0$ used in [17].

Finally, we consider the transformations in the elliptic conjugacy class of the form

$$\mathcal{M} = \begin{pmatrix} \cos\left(\frac{kz}{2}\right) & \sin\left(\frac{kz}{2}\right) \\ -\sin\left(\frac{kz}{2}\right) & \cos\left(\frac{kz}{2}\right) \end{pmatrix}. \tag{A.4}$$

After writing $\phi_0 = \varphi_0$ we find that this induces the transformation

$$\chi \to \frac{\sinh \varphi_0 \, \sin kz}{\cosh \varphi_0 + \sinh \varphi_0 \, \cos kz} \,,$$

$$e^\phi \to \cosh \varphi_0 + \sinh \varphi_0 \, \cos kz \,. \tag{A.5}$$

This generates $\varphi = \varphi(r)$, and $\alpha = k\,z$, exactly as in (2.6) and (3.1). Notice that as we traverse once in the Poincaré disc via $z \to z + 2\pi/k$, we see from (A.4) that we move from $\mathcal{M} = 1$ to $\mathcal{M} = -1$. In other words we have a closed orbit in PSL$(2, R)$.

References

[1] J.M. Maldacena, *The Large-N limit of superconformal field theories and supergravity*, *Int. J. Theor. Phys.* **38** (1999) 1113 [hep-th/9711200] [INSPIRE].

[2] I.R. Klebanov and E. Witten, *Superconformal field theory on three-branes at a Calabi-Yau singularity*, *Nucl. Phys.* **B 536** (1998) 199 [hep-th/9807080] [INSPIRE].

[3] J.P. Gauntlett, D. Martelli, J. Sparks and D. Waldram, *Sasaki-Einstein metrics on $S^2 \times S^3$*, *Adv. Theor. Math. Phys.* **8** (2004) 711 [hep-th/0403002] [INSPIRE].

[4] S. Benvenuti, S. Franco, A. Hanany, D. Martelli and J. Sparks, *An Infinite family of superconformal quiver gauge theories with Sasaki-Einstein duals*, *JHEP* **06** (2005) 064 [hep-th/0411264] [INSPIRE].

[5] S.A. Hartnoll and D.M. Hofman, *Locally Critical Resistivities from Umklapp Scattering*, *Phys. Rev. Lett.* **108** (2012) 241601 [arXiv:1201.3917] [INSPIRE].

[6] G.T. Horowitz, J.E. Santos and D. Tong, *Optical Conductivity with Holographic Lattices*, *JHEP* **07** (2012) 168 [arXiv:1204.0519] [INSPIRE].

[7] A. Donos and S.A. Hartnoll, *Interaction-driven localization in holography*, *Nature Phys.* **9** (2013) 649 [arXiv:1212.2998] [INSPIRE].

[8] A. Donos and J.P. Gauntlett, *Holographic Q-lattices*, *JHEP* **04** (2014) 040 [arXiv:1311.3292] [INSPIRE].

[9] T. Andrade and B. Withers, *A simple holographic model of momentum relaxation*, *JHEP* **05** (2014) 101 [arXiv:1311.5157] [INSPIRE].

[10] A. Donos and J.P. Gauntlett, *Novel metals and insulators from holography*, *JHEP* **06** (2014) 007 [arXiv:1401.5077] [INSPIRE].

[11] B. Goutéraux, *Charge transport in holography with momentum dissipation*, *JHEP* **04** (2014) 181 [arXiv:1401.5436] [INSPIRE].

[12] T. Azeyanagi, W. Li and T. Takayanagi, *On String Theory Duals of Lifshitz-like Fixed Points*, *JHEP* **06** (2009) 084 [arXiv:0905.0688] [INSPIRE].

[13] D. Mateos and D. Trancanelli, *The anisotropic N = 4 super Yang-Mills plasma and its instabilities*, *Phys. Rev. Lett.* **107** (2011) 101601 [arXiv:1105.3472] [INSPIRE].

[14] D. Mateos and D. Trancanelli, *Thermodynamics and Instabilities of a Strongly Coupled Anisotropic Plasma*, *JHEP* **07** (2011) 054 [arXiv:1106.1637] [INSPIRE].

[15] E. Banks and J.P. Gauntlett, *A new phase for the anisotropic $N = 4$ super Yang-Mills plasma*, *JHEP* **09** (2015) 126 [arXiv:1506.07176] [INSPIRE].

[16] E. Banks, *Phase transitions of an anisotropic $N = 4$ super Yang-Mills plasma via holography*, *JHEP* **07** (2016) 085 [arXiv:1604.03552] [INSPIRE].

[17] S. Jain, N. Kundu, K. Sen, A. Sinha and S.P. Trivedi, *A Strongly Coupled Anisotropic Fluid From Dilaton Driven Holography*, *JHEP* **01** (2015) 005 [arXiv:1406.4874] [INSPIRE].

[18] P. Chesler, A. Lucas and S. Sachdev, *Conformal field theories in a periodic potential: results from holography and field theory*, *Phys. Rev.* **D 89** (2014) 026005 [arXiv:1308.0329] [INSPIRE].

[19] A. Donos, J.P. Gauntlett and C. Pantelidou, *Conformal field theories in $d = 4$ with a helical twist*, *Phys. Rev.* **D 91** (2015) 066003 [arXiv:1412.3446] [INSPIRE].

[20] G.T. Horowitz and M.M. Roberts, *Zero Temperature Limit of Holographic Superconductors*, *JHEP* **11** (2009) 015 [arXiv:0908.3677] [INSPIRE].

[21] P. Basu, J. He, A. Mukherjee and H.-H. Shieh, *Hard-gapped Holographic Superconductors*, *Phys. Lett.* **B 689** (2010) 45 [arXiv:0911.4999] [INSPIRE].

[22] A. Donos, J.P. Gauntlett and C. Pantelidou, *Competing p-wave orders*, *Class. Quant. Grav.* **31** (2014) 055007 [arXiv:1310.5741] [INSPIRE].

[23] S. Harrison, S. Kachru and H. Wang, *Resolving Lifshitz Horizons*, *JHEP* **02** (2014) 085 [arXiv:1202.6635] [INSPIRE].

[24] J. Bhattacharya, S. Cremonini and A. Sinkovics, *On the IR completion of geometries with hyperscaling violation*, *JHEP* **02** (2013) 147 [arXiv:1208.1752] [INSPIRE].

[25] N. Kundu, P. Narayan, N. Sircar and S.P. Trivedi, *Entangled Dilaton Dyons*, *JHEP* **03** (2013) 155 [arXiv:1208.2008] [INSPIRE].

[26] J. Bhattacharya, S. Cremonini and B. Goutéraux, *Intermediate scalings in holographic RG flows and conductivities*, *JHEP* **02** (2015) 035 [arXiv:1409.4797] [INSPIRE].

[27] A. Donos, J.P. Gauntlett and C. Pantelidou, *Semi-local quantum criticality in string/M-theory*, *JHEP* **03** (2013) 103 [arXiv:1212.1462] [INSPIRE].

[28] G. Policastro, D.T. Son and A.O. Starinets, *The Shear viscosity of strongly coupled $N = 4$ supersymmetric Yang-Mills plasma*, *Phys. Rev. Lett.* **87** (2001) 081601 [hep-th/0104066] [INSPIRE].

[29] P. Kovtun, D.T. Son and A.O. Starinets, *Viscosity in strongly interacting quantum field theories from black hole physics*, *Phys. Rev. Lett.* **94** (2005) 111601 [hep-th/0405231] [INSPIRE].

[30] A. Rebhan and D. Steineder, *Violation of the Holographic Viscosity Bound in a Strongly Coupled Anisotropic Plasma*, *Phys. Rev. Lett.* **108** (2012) 021601 [arXiv:1110.6825] [INSPIRE].

[31] K.A. Mamo, *Holographic RG flow of the shear viscosity to entropy density ratio in strongly coupled anisotropic plasma*, *JHEP* **10** (2012) 070 [arXiv:1205.1797] [INSPIRE].

[32] R. Critelli, S.I. Finazzo, M. Zaniboni and J. Noronha, *Anisotropic shear viscosity of a strongly coupled non-Abelian plasma from magnetic branes*, *Phys. Rev.* **D 90** (2014) 066006 [arXiv:1406.6019] [INSPIRE].

[33] S. Jain, R. Samanta and S.P. Trivedi, *The Shear Viscosity in Anisotropic Phases*, *JHEP* **10** (2015) 028 [arXiv:1506.01899] [INSPIRE].

[34] J. Erdmenger, P. Kerner and H. Zeller, *Non-universal shear viscosity from Einstein gravity*, *Phys. Lett.* **B 699** (2011) 301 [arXiv:1011.5912] [INSPIRE].

[35] A. Donos and J.P. Gauntlett, *Thermoelectric DC conductivities from black hole horizons*, *JHEP* **11** (2014) 081 [arXiv:1406.4742] [INSPIRE].

[36] A. Donos and J.P. Gauntlett, *Navier-Stokes Equations on Black Hole Horizons and DC Thermoelectric Conductivity*, *Phys. Rev.* **D 92** (2015) 121901 [arXiv:1506.01360] [INSPIRE].

[37] E. Banks, A. Donos and J.P. Gauntlett, *Thermoelectric DC conductivities and Stokes flows on black hole horizons*, *JHEP* **10** (2015) 103 [arXiv:1507.00234] [INSPIRE].

[38] A. Donos, J.P. Gauntlett, T. Griffin and L. Melgar, *DC Conductivity of Magnetised Holographic Matter*, *JHEP* **01** (2016) 113 [arXiv:1511.00713] [INSPIRE].

[39] S.A. Hartnoll and E. Shaghoulian, *Spectral weight in holographic scaling geometries*, *JHEP* **07** (2012) 078 [arXiv:1203.4236] [INSPIRE].

[40] S. Benvenuti and A. Hanany, *Conformal manifolds for the conifold and other toric field theories*, *JHEP* **08** (2005) 024 [hep-th/0502043] [INSPIRE].

[41] L. Cheng, X.-H. Ge and S.-J. Sin, *Anisotropic plasma at finite U(1) chemical potential*, *JHEP* **07** (2014) 083 [arXiv:1404.5027] [INSPIRE].